Indian Journal of Pure & Applied Physics
Vol. 59, February 2021, pp. 143-149

Chemically synthesized Bi_2S_3, CuS and Bi_2S_3/CuS heterostructure materials as counter electrode: Dye sensitized solar cell application

Shital M Sonar[a], Prashant K Baviskar[b], Habib M Pathan[c] & Prakash B Ahirrao[a*]

[a]Department of Physics, S V S's Dadasaheb Rawal College, Dondaicha – 425 408

[b]Department of Physics, SN Arts, DJ Malpani Commerce and BN Sarda Science College, Sangamner 422605, (M S), India

[c]Advanced Physics Laboratory, Department of Physics, Savitribai Phule Pune University, Pune – 411 007, (M S), India

Received 8 September 2020; accepted 9 November 2020

In the present work, we have successfully synthesized Bi_2S_3, CuS, and its heterojunction Bi_2S_3/CuS thin film on fluorine doped tin oxide (FTO) coated glass as counter electrodes. These depositions are done by simple, cost effective, and simply executable sequential chemical bath deposition (S-CBD) method. Well optimized preparative parameters led to the formation of good quality thin films of Bi_2S_3 and CuS films and heterojunction. The structural validation Bi_2S_3, CuS, and its heterojunction were achieved by X-ray diffraction and Raman scattering, surface morphological study observed through Scanning Electron Microscopy (SEM) and topology was confirmed by Atomic Force Microscopy (AFM). We have employed Bi_2S_3/CuS heterostructure as a counter electrode (CE) in dye-sensitized solar cell (DSSC). We have observed different parameters like short circuit current density (Jsc), open circuit voltage (Voc), Fill Factor (FF) and efficiency (n) by Current–voltage (J-V) characteristics. Though we do not achieve an anticipated outcome for heterostructure compared with conventional Platinum and Carbon black counter electrode, CuS separately found worthy as Counter electrode (CE) in DSSC.

Keywords: Bi_2S_3, CuS, Heterostructure, sequential chemical bath deposition, Counter electrode, Solar cell.

1 Introduction

Generation of energy by simple, efficient way and at low cost is a crucial part of today's technological era as energy demand is continuously increasing with time. To fulfill the requirement of energy ample efforts done with various renewable sources of energy like wind, hydropower and solar energy. Among from that Sun energy is found to be most suitable source as wind and hydropower need sophisticated and high-cost for generation of electricity[1, 2] while solar energy can directly use to convert into electricity by using the solar cell.[3] Solar cells seems to be an unpolluted, promising, safe and affordable source of renewable energy and hence used in various progressive forms like Silicon solar cells, Quantum dot solar cells (QDSSC), Dye sensitized solar cells (DSSC), and Perovskite solar cells. More specifically talking, Dye Sensitized Solar Cell (DSSC) has specific consideration due to its noticeable advantages like easier device fabrication, better efficiency, flexibility, environment friendly[4, 5]. The performance of DSSC is based on all of its constituents like Photoanode, light-absorbing dye, an electrolyte possessing a redox couple (I_3^-/ I^-) and counter electrode (CE). The CE is an obligatory element in DSSC and requires high catalytic activity, high conductivity and high reflectivity. These are needed properties to stimulate redox couple reaction by electron recombination, to improve electron transport, and to return unabsorbed light energy to the solar cell device[6, 7]. In recent times, there are number of materials act as a counter electrodes in DSSCs reported in literatures such as carbon black[8], carbon nanotubes[9], transition metal sulphides like titanium disulphide[10] , cobalt sulphide[11], nickel sulphide[11,12], molybdenum sulphide[13], graphene-mediated MoS_2 nanosheets[14], transition metal carbides[15], transition metal nitrides[16], Platinum (Pt) and carbon were standard CE materials from long time in DSSC as they are having high catalytic and good conductive properties[17,18]. Due to high cost of platinum and unstable performance with redox liquid electrolyte there is need to find replacement. Herein we have tried to synthesize Bismuth sulphide (Bi_2S_3), Copper sulphide (CuS) and its heterojunction Bi_2S_3/CuS films by using low cost and easier sequential chemical bath deposition (S-CBD) method.

It is perceived that Bi_2S_3 shows a good performance in DSSCs as a CE material, due to its

*Corresponding author (E-mail: ahirraoprakash@gmail.com)

low direct band gap of 1.2–1.7 eV, an absorption coefficient in the order of 10^4–10^5 cm^{-1} and an appreciable conversion efficiency[19]. Its heterojunction like Bi_2S_3–C microsphere synthesized by a facile one-step solvothermal method gives a high conversion efficiency of 6.72 % by optimizing carbon content in composite materials[20]. Mesoporous Bi_2S_3 nanorods mixed with graphene oxide used as CE in DSCs and it found to be an efficient alternative to Pt[21]. p-Cu_2CdSnS_4 (p-CCTS)/n-Bi_2S_3 heterojunction photodiode showed a good rectifying behavior and it is concluded that the CdS material in traditional thin film PV devices can be replaced with Bi_2S_3 for better transportation of charge carriers in the PN-junction[22]. Moving further considering Copper sulphide (CuS) which occurs in five phases such as covellite (CuS), anilite ($Cu_{1.75}S$), digenite ($Cu_{1.8}S$), djurleite ($Cu_{1.95}S$) and chalcocite (Cu_2S),respectively due to different stoichiometric ratios of copper and sulfur source[23]. The band gap of CuS has values ranging from 1.2 eV to 2 eV (for the "copper-rich" phase to for "copper-deficient" phase) [24-26]. Before this Copper sulphide (CuS) in its dignite phase $Cu_{1.8}S$[27] reported as counter electrode in DSSC. CuSe and CuS were comparatively studied as CE in QDSSC with platinum as a standard CE[28].

In this proposed work we demonstrated about synthesis of chalcogenide metal sulphide thin films of Bi_2S_3,CuS and Bi_2S_3/CuS heterojunction as counter electrode, synthesized by Sequential chemical bath deposition method (S-CBD).To the best of our knowledge for the first time Bi_2S_3/CuS heterojunction is tested as CE in DSSC towards Pt and carbon free counter electrode in DSSC.

2 Experimental Specifics

2.1 Chemicals

Bismuth (III) nitrate Bi $(NO_3)_2.5H_2O$ and Sodium sulfide ($Na_2S{\cdot}xH_2O$) (Sigma Aldrich).Copper sulfate pentahydrate ($CuSO_4.5H_2O$), ammonia (25%), Sodium sulfide ($Na_2S{\cdot}xH_2O$) (SRL). ZnO powder (Sigma Aldrich), Ethyl cellulose (SDFCL), α-terpenol (HPCL), acetyl acetone (SRL) was used to form ZnO films. Mercurochrome dye (Sigma Aldrich) was used as a sensitizer over ZnO films to form photoanode. All these chemicals purchased are of analytical grade and were used as received without any purification.

2.2 Synthesis of Bi_2S_3, CuS and Bi_2S_3/CuS heterojunction counter electrode

In this present work, the deposition of Bi_2S_3, CuS, and Bi_2S_3 /CuS heterojunction have done by a very simple Sequential chemical bath deposition method (S-CBD) method. S-CBD method involves immersion of substrate into cationic and anionic precursors placed in different beakers along with that distilled water for intermediate rinsing purpose to avoid inhomogeneous precipitation. Schematic representation of S-CBD method for the deposition of Bi_2S_3, CuS, and Bi_2S_3 /CuS heterojunctions is shown in Fig. 1. This deposition is similar to that of Successive Ionic Layer Adsorption and Reaction (SILAR)[29], which takes place by atomic layer by atomic layer so thickness can be controlled easily by varying the S-CBD cycles. The cationic precursor was 0.003 M aqueous solution of bismuth nitrate [Bi $(NO_3)_2$] complexed with triethanolamine (TEA). The pH of this solution was maintained at 9. The anionic precursor was 0.015 M of sodium sulphide [Na_2S] with pH maintained at 10. For the deposition of Bi_2S_3 thin films, a well cleaned fluorine doped tin oxide (FTO) coated glass substrate was immersed in cationic precursor solution of bismuth nitrate [$Bi(NO_3)_2$] for 20 sec.in which Bi^{3+} ions are adsorbed on the surface of the substrate. The substrate was rinsed with double distilled water for 20 sec. to remove unadsorbed ions. The substrate was then immersed in an anionic precursor of sodium sulphide solution for 20 sec in which S^{2-} ions are reacted with adsorbed Bi^{3+} ions on the substrate. This was followed by rinsing again in double distilled water for 20 sec. to remove unreacted S^{2-} ions. This completes one deposition cycle for the deposition of Bi_2S_3 thin films. By repeating such deposition cycles for 60 times, continuous brown coloured, shiny, mirror-like Bi_2S_3 film obtained on the substrate. The deposition was carried out at room temperature (303K).The as-deposited thin film of Bi_2S_3 then annealed at 473K for 1 hour in furnace.

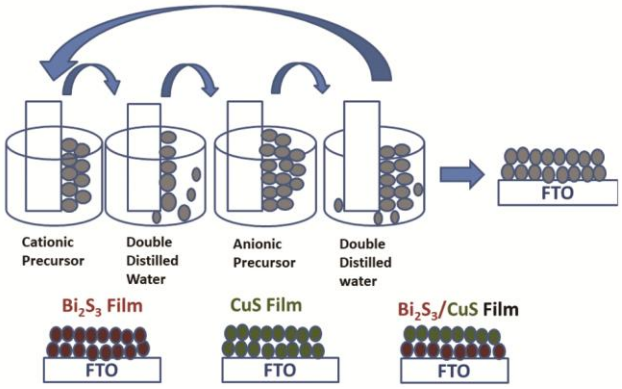

Fig. 1 — Schematic representation of S-CBD method for the deposition of Bi_2S_3, CuS and Bi_2S_3 /CuS heterojunctions.

An equimolar (0.05 M) cationic and anionic precursor of copper sulphate ($CuSO_4$) and sodium sulphide (Na_2S) was taken. Well cleaned FTO glass substrate is immersed in cationic precursor for 10 sec in which Cu^{2+} ions are adsorbed on the surface of the substrate and then rinsed in double distilled water for 20 sec to remove loosely bound ions. The substrate was then immersed in an anionic precursor of sodium sulphide solution for 10 sec in which S^{2-} ions are reacted with adsorbed Cu^{2+} ions on the FTO .This was followed by rinsing again in double distilled water for 20 sec to remove unreacted S^{2-} ions. This completes one cycle of deposition. Such 60 S-CBD cycles were done and then this FTO is kept for annealing in furnace for 1 hour at 473K.

For the deposition of heterojunction film, the annealed film of Bi_2S_3 is considered as substrate and it is used in equimolar cationic and anionic precursors of copper sulphate ($CuSO_4$) of 0.05 M and sodium sulphide (Na_2S) of 0.05 M respectively. The substrate immersed in cationic precursor for 10 sec in which Cu^{2+} ions are adsorbed on the surface of the substrate and then rinsed in double distilled water for 20 sec to remove loosely bound ions. The substrate was then immersed in an anionic precursor of sodium sulphide solution for 10 sec in which S^{2-} ions are reacted with adsorbed Cu^{2+} ions on the FTO. In this way one cycle of deposition is completed and CuS thin film starts depositing over Bi_2S_3 thin film. After completing 60 S-CBD cycles heterojunction film is ready and kept it for air annealing at 473K for 1 hour.

2.3 Synthesis of ZnO Photoanode

Photoanode is a very crucial part of DSSC. Well cleaned FTO of resistance ~10 Ω/cm^2 were used to deposit ZnO thin film by the doctor blade technique. Initially, compact layer of ZnO is formed on FTO glass substrates by S-CBD at room temperature followed by deposition of mesoporous ZnO film by the doctor blade technique. The film is then dried at 333K and then annealed in an air furnace at 723K for 1 hour. Annealed ZnO films dipped into the 500 µM mercurochrome (MC) dye solution. To get the desired dye absorbed on photoanodes it is kept inside dye for 72 h at room temperature under dark condition. After 72 hours the photoanode was take outside and washed with ethanol to remove the excess amount of dye and then dried it at room temperature[30].

2.4 Device fabrication

The DSSC was fabricated with FTO/ZnO photoanode sensitized with mercurochrome dye, polyiodide as an electrolyte, and Bi_2S_3, CuS, Bi_2S_3/CuS heterojunction as counter electrodes along with standard Carbon black and Platinum CEs. During assembly of the solar cell, photoanode and counter electrode were clamped together with binder clips, a small quantity of polyiodide electrolyte introduced between two electrodes by capillary action.

3 Characterizations

The crystal structure of annealed Bi_2S_3 thin film, CuS thin film, and heterojunction Bi_2S_3/CuS were evaluated by X-ray diffractometer (XRD Rigaku D/ max-2400 with Cu-k_α radiation (λ= 0.154 nm) in the range of 20^o-80^o. The surface morphology and structure of the samples were analyzed by field emission scanning electron microscopy (FESEM: Nova NanoSEM NPEP303) with accelerating voltage 10-15 KV, furnished with an energy dispersive X-ray spectrometer (EDX). EDX study gives details about the elemental composition of prepared samples. Raman spectroscopy was directed using a In Via Micro RAMAN (Reni Shaw) spectrophotometer with 532 nm laser excitation at room temperature to confirm the presence of vibration mode of Bi_2S_3, CuS, Bi_2S_3-CuS samples. Atomic force microscopy (AFM) study was done by using Nanoscope IIIa provided by Vecco digital instruments to know about the surface roughness of the samples. The photocurrent density–voltage (J–V) measurements were carried out on a Keithley 2400 digital source meter under AM 1.5G illumination. All the measurements were recorded at room temperature.

4 Results and Discussions

Structural study

We can explore the structural properties and crystallinity of prepared samples by performing an X-ray diffraction (XRD) study. As X-ray diffraction (XRD) implemented, patterns of bare Bi_2S_3, CuS, and Bi_2S_3/CuS heterojunction are shown in Fig. 2. The diffraction peaks are indexed by a star symbol corresponding to the FTO glass substrate. XRD pattern of Bi_2S_3 depicts sharp peaks observed at 2θ = 22.50^o, 23.70^o, 25.01^o, 28.61^o, 31.82^o, 39.9^o, 46.5^o, and 52.66^o which corresponds to (220), (101), (100), (211), (221), (141), (431) and (351) lattice planes strongly confirms the orthorhombic structure of Bi_2S_3[31] and in good synchronization with JCPDS card no. 17-0320. XRD profile of CuS shows prominent peaks at 2θ = 29.21^o, 31.82^o, 47.95^o with corresponding lattice planes at (102), (103) and (110)

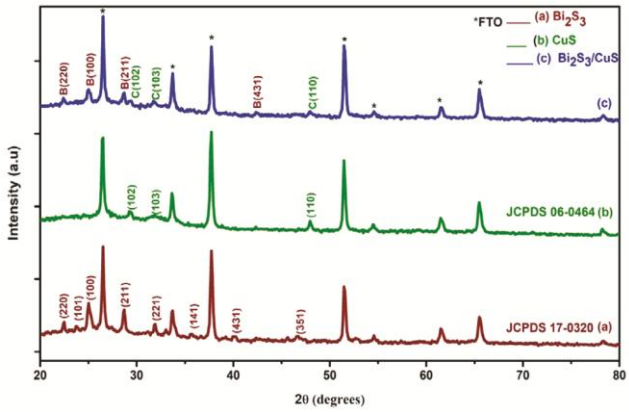

Fig. 2 — XRD patterns of Bi_2S_3, CuS and Bi_2S_3/CuS film on FTO substrate.

respectively, which confirms hexagonal covellite structure of CuS[32] and good agreement with JCPDS card no. 06-0464. The average crystallite size of the deposited layer of Bi_2S_3 is calculated by Debye–Scherrer`s formula applied at an angle 25.01° is 20 nm and for CuS it is applied at an angle 33.62° and size is found to be 33 nm. Bi_2S_3/CuS heterojunction XRD pattern depicts that shift in peaks due to heterojunction surface and wider peaks as the collective effect of reflection from Bi_2S_3 and CuS layer. XRD pattern of heterojunction Bi_2S_3/CuS shows a drop of intensity in Bi_2S_3 diffraction peaks than that of CuS diffraction peaks. No peaks from other phases have been spotted, signifying that the heterojunction was highly purified.

Raman spectra

The Raman spectrum of the annealed Bi_2S_3, CuS, and Bi_2S_3/CuS thin film films recorded between 0-1000 cm^{-1} ranges. Figure 3 displays four characteristic vibrational peaks appearing in the A_g mode at 99.9, 189, 237.6 cm^{-1}, and the B_{1g} mode 262.2 cm^{-1}.These peaks synchronize well with the Bi_2S_3 Raman bands as reported in literature[33]. In Fig. 3 a very sharp Raman peak observed around 473.1 cm^{-1} in the high-frequency region due to lattice vibration of CuS and a less prominent peak at 266 cm^{-1} [34]. These peaks corresponding to A_{1g} longitudinal optical (LO) mode, and A_{1g} transverse optical (TO) respectively[32]. The sharp peak of 473.1 cm^{-1} is recognized as due to the S–S stretching mode of S_2 ions[35]. Bi_2S_3/CuS heterosturcture show Bi_2S_3 characteristic reflection peaks A_g and B_{1g} mode at 264.2 and 292.2 cm^{-1} respectively also CuS A_{1g} transverse optical (TO) peak observed at 264.2 cm^{-1} and A_{1g} longitudinal optical (LO) mode shift at 475 cm^{-1}. Black vertical lines shows the shifting of Raman vibration mode in

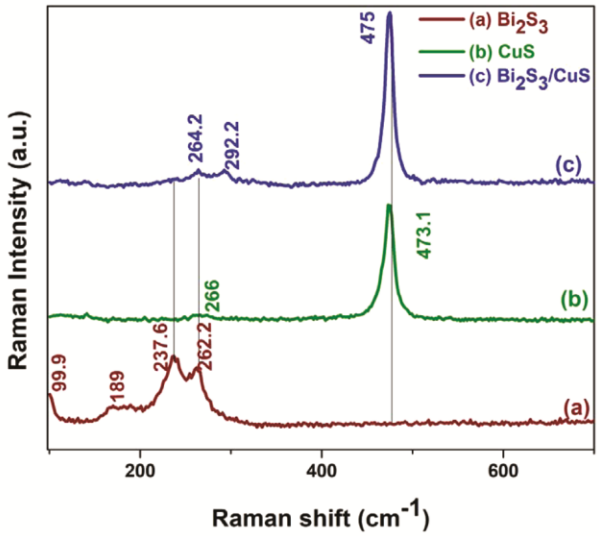

Fig. 3 — Raman Spectrum of Bi_2S_3, CuS and Bi_2S_3/CuS heterojunction.

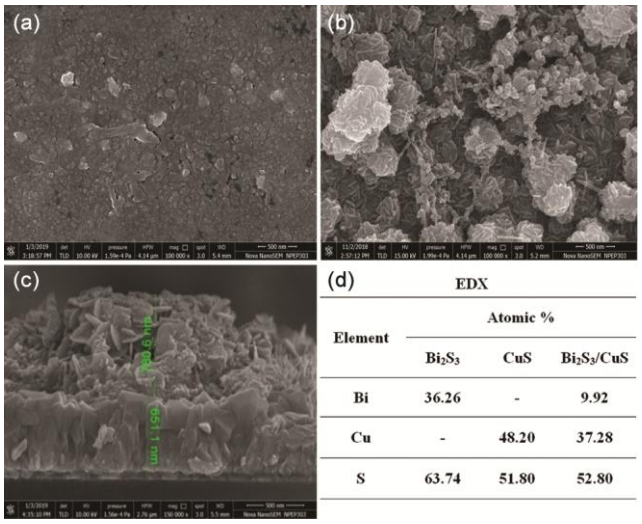

Element	Atomic %		
	Bi_2S_3	CuS	Bi_2S_3/CuS
Bi	36.26	-	9.92
Cu	-	48.20	37.28
S	63.74	51.80	52.80

Fig. 4 — FESEM images of (a) Bi_2S_3 (b) CuS (c) cross sectional view of Bi_2S_3/CuS and (d) Elemental composition of above mentioned film by EDX mapping.

Bi_2S_3/CuS heterojunction is stable with prior studies and supports the interaction between Bi_2S_3 [33] and CuS[34].

Morphological and cross-sectional study

Scanning Electron Microscopy was carried to explore morphological studies of film deposited on substrate. It also helps to observe uniformity, smoothness and nature of the films. Figure 4 shows scanning electron micrograph for bare Bi_2S_3, CuS and Bi_2S_3/CuS heterojunction. For bare Bi_2S_3 Fig. 4(a) with higher magnification shows films appear to be homogeneous surface of spherical nanograins with dense concentration, without void and adhesive well

with substrate[36]. In case of CuS Fig. 4(b) with higher magnification shows several plates gathered to form flower like nanostructures owing to roughness to its structure with well coverage on the substrate surface[37]. This roughness helps to provide more contact area to electrolyte useful for electron conduction. Cross-sectional view in Fig. 4(c) with 150,000x magnification clearly shows the compact and void free deposition of two different films with different morphologies. Lower Bi_2S_3 film has thickness 651.1 nm and CuS film have 780.6 nm thicknesses. The purity and chemical composition of the Bi_2S_3, CuS and Bi_2S_3/CuS films were further acknowledged by means of energy-dispersive X-ray spectroscopy (EDX) attached to the SEM. In Bi_2S_3 film the molar ratio of Bi:S is measured by EDX to be approximately 2:3, is in good agreement with stoichiometry of Bi_2S_3. In case of CuS the molar ratio of Cu:S is to be approximately 1:1, this also in concurrent with stoichiometric covellite CuS. In Bi_2S_3/CuS heteojunction it is observed from EDX that presence of this is sulphur rich as both films individually have sulphur content. It confirms the presence of expected elements in anticipated atomic percentages and was tabulated in table as shown in Fig. 4(d).

Atomic Force Microscopic Study

Atomic Force Microscopy (AFM) is an excellent technique to study the topology and texture of different surfaces. Figure 5 shows the surface morphology of Bi_2S_3, CuS and Bi_2S_3/CuS thin film respectively. Figure 5(a) taken at a 5µm x 5µm scan are shows a granular, polycrystalline uniform morphology; it also observed that smaller aggregates combine to form larger ones and the substrate surface is well covered by closely packed spherical or elliptical aggregates in the form of hillocks. The aggregates are distinct and uniform[38]. Figure 5(b) shows CuS thin film morphology taken at 5µm x 5µm scan area. It displays the presence of highly co-ordinated smaller grains that are well adhered to substrate surface[39]. Figure 5(c) displays the morphology of Bi_2S_3/CuS thin film heterojunction taken at 5 µm x 5 µm scan area. It shows the heterojunction sample shows a combination of few hillocks with smooth surface as compared to individual surfaces. Figure 5(b) shows 2-D AFM images of Bi_2S_3, CuS, and Bi_2S_3/CuS films which show topology are highly consistent with SEM results.

Photovoltaic performance

Figure 6(a) Schematic representation of DSSC operation with different CE and (b) highlights photocurrent density–voltage (J-V) plots of DSSC presenting Pt, Carbon, Bi_2S_3, CuS, and Bi_2S_3/CuS counter electrode. Table 1 shows the detailed parameters evaluation of different CEs using synthesized DSSC. Under the illumination of 1 sun, Bi_2S_3 CE based DSSC gave power energy conversion efficiency of 0.13%, CuS CE showed energy conversion efficiency of 0.41% which is comparable

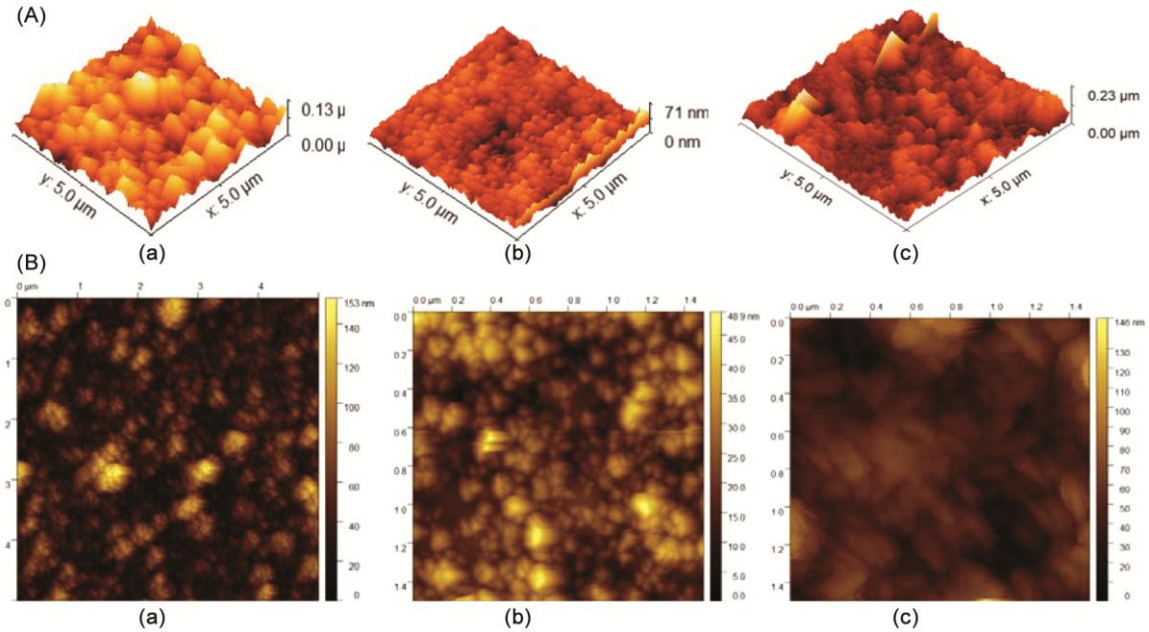

Fig. 5 — (A)3D AFM images (a) Bi_2S_3 (b) CuS and (c) Bi_2S_3/CuS heterojunction (B) 2D AFM images (a) Bi_2S_3 (b) CuS and (c) Bi_2S_3/CuS heterojunction.

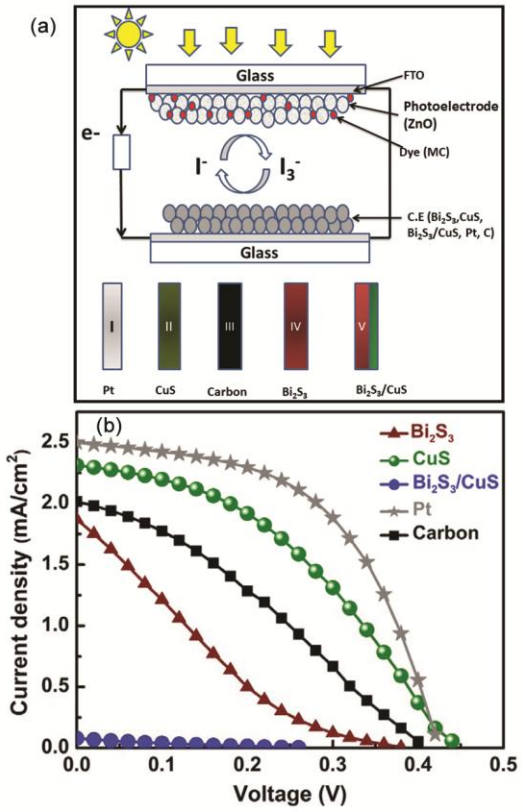

Fig. 6 — (a) Schematic representation of DSSC structure and (b) J–V curves of FTO/ZnO/dye/electrolyte/different CE's

Table 1 — FTO/ZnO/dye/electrolyte/CE's device performance with various CE's.

C.E	V_{oc} (V)	J_{sc} (mA/cm^2)	FF (%)	Efficiency (%)
Bi_2S_3	0.38	1.87	18	0.13
CuS	0.43	2.31	41	0.41
Bi_2S_3/CuS	0.27	0.08	18	0.004
Platinum	0.42	2.49	53	0.56
Carbon	0.40	2.01	32	0.26

with the Pt and Bi_2S_3/CuS heterojunction as CE gives poor performance with0.004% efficiency. DSSC with conventional CE that is Pt has energy conversion efficiency (η) of 0.56% whereas Carbon gives 0.26%. The small value of η for Bi_2S_3/CuS heterojunction is mainly owing to poorer electrocatalytic activity Bi_2S_3/CuS heterojunction electrode for a polyiodide redox reaction. It is manifested from the output that though the efficiency of Bi_2S_3 and CuS as CE appears to be comparably low as that of Pt, but it has scope for further improvement in charge transfer at the CE/electrolyte interface by changing appropriate preparative parameters. CuS based CE in DSSC has power conversion efficiency PCE 5.03% [30]. As compared to carbon CE, CuS gives an appreciable improvement in efficiency so it could be a good alternative for Carbon CE in DSSC.

Conclusion

In this study via a simple but very proficient chemical method we successfully synthesize Bi_2S_3, CuS, and Bi_2S_3/CuS heterojunction thin films. This facile synthesis method produces a thin layer Bi_2S_3, CuS, and Bi_2S_3/CuS on FTO with good adhesion which is an important factor. We have examined bottom layer Bi_2S_3 and top layer CuS Properties separately and discuss them in detail. By studying Current density-Voltage (J-V) plots we can conclude about the electrocatalytic activity of CEs. Bi_2S_3/CuS heterojunction as CE reveals very poor response so it cannot be a potential candidate for CE in DSSC. Whereas CuS CE revealed a power conversion efficiency of 0.41% which is appreciably better than carbon (0.26%) CE and close to Pt efficiency (0.56%). It confirms that cost effective CuS comes out to be a better alternative for Pt and Carbon in DSSC.

Acknowledgements

SMS and PBA are thankful to Principal, S.V.S.'s Dadasaheb Rawal College, Dondiacha for support and lab facility. HMP is thankful to DST, New Delhi, for financial support [DST/TMD/SERI/S173(C)].

References

1 Wurfel P, *Physics of Solar Cells: From Principles to New Concepts*, (2005) WILEY-VCH Verlag GmbH & Co. KGaA
2 Poudel P & Qiao Q, *Nanoscale*, 4 (2012) 2826.
3 Lewis N S, *Science*, 315 (2007) 798.
4 Brabec C J, Hauch J A, Schilinsky P & Waldauf C, *MRS Bull*, 30 (2005) 50.
5 Gregg B A, *MRS Bull*, 30 (2005) 20.
6 Wang L, Al-Mamun M & Liu P, NPG *Asia Mater*, 7 (2015) e226.
7 Wu J, Li Y & Tang Q, *Sci Rep*, 4 (2015) 4028.
8 Rose I R C & Rajendran A J, *Optik*, 155 (2018) 63.
9 Lee W J, Ramasamy E, Lee D Y & Song J S, *ACS Appl Mater Interfaces*, 21 (2009) 1145.
10 Meng X, Yu C, Lu B, Yang J & Qiu J, *Nano Energy*, 22 (2016) 59.
11 Kung W, Chen H W & C Y Lin, *ACS Nano*, 6 (2012) 7016.
12 Sun H, Qin D, Huang S, *Energy Environ Sci*, 4 (2011) 2630.
13 Vikraman D, Arbab A & Hussain S, *ACS Sustainable Chem Eng*, 7 (2019) 13195.
14 Yu C, Meng X & Song X, *Carbon*, 100 (2016) 474.
15 Wu M, Lin X, Hagfeldt A & Ma T, *Angewandte Chem Int Edn*, 50 (2011) 3520.
16 Song J, Li G R, Xi K & Lei B, *J Mater Chem A*, 2 (2014) 10041.
17 Kakiage K, Aoyama Y & Yano T, *Chem Commun*, 51 (2015) 88.

18 Kumar R, Sahajwallab V & Bhargava P, *Nanoscale Adv*, 1 (2019) 3192.
19 Peter L M, Wijayantha K G U, Riley D J & Waggett J P, *J Phys Chem B*, 107 (2003) 8378.
20 Zuo X, Yang X, Zhou L & Yang B, *RSC Adv*, 4 (2014) 57412.
21 Sheng-Qi G, Tian-Zeng J & Xiao Z, *Nanoscale*, 6 (2014) 14433.
22 Kumar M S, Madhusudanan S P, Mohanta K & Batabya S K, *Mater Res Express*, 7 (2020) 015909.
23 Vasquez Y, Fenton E M, Chernow V F & Aizenberg J, *Cryst Eng Commun*, 13 (2011) 1077.
24 Goble R J, *Can Mineralogist*, 23 (1985) 61.
25 Shinde M S, Ahirrao P B & Patil I J, *Indian J Pure Appl Phys*, 50 (2012) 657.
26 Klimov V I, Bolivar P H & Karavanskii V A, *Superlattices Microstruct*, 20 (1996) 395.
27 Mulmudi H, Batabyal S & Rao M, *Phys Chem Chem Phys*, 13 (2011) 19307.
28 Palve B M, Kadam V S & Jagtap C V, *J Mater Sci Electron*, 28 (2017) 14394.
29 Pathan H M & Lokhande C D, *Bull Mater Sci*, 27 (2004) 85.
30 Baviskar P K, Dubal D P & Majumder S, *J Photochem Photobio A: Chem*, 318 (2016) 135.
31 Moreno-Garcíaa H, Messina S, Calixto-Rodriguezc M & Martínez H, *Appl Surf Sci*, 311 (2014) 729.
32 Marimuthu T, Anandhan N & Panneerselvam R, *Nano-Structures Nano-Objects*, 17 (2019) 138.
33 Zhao Y, Chua K T E, Gan C K, *Phys Rev B*, 84 (2011) 205330.
34 Ishii M, Shibata K & Nozaki H, *J Solid State Chem*, 105 (1993) 504.
35 Thongtem T, Phuruangra A & Thongtem S, *J Mater Sci*, 42 (2007) 93.
36 Ahire R R, Sankapal B R & Lokhande C D, *MRS Bull*, 36 (2001) 199.
37 Shinde M S & Patil R S, *Int J Chem Phys Sci*, 3 (2014).
38 Mageshwari K & Sathyamoorthy R, *Mater Sci Semicond Process*, 16 (2013) 43.
39 Sagade A A & Sharma R, *Sensor Actuator B Chem*, 133 (2008) 135.